Available online at www.sciencedirect.com
SCIENCE DIRECT®
Journal of volcanology and geothermal research
ELSEVIER
Journal of Volcanology and Geothermal Research xx (2006) xxx–xxx
www.elsevier.com/locate/jvolgeores

# Azores hotspot signature in the upper mantle

Graça Silveira [a,b,*], Eléonore Stutzmann [c], Anne Davaille [c], Jean-Paul Montagner [c], L. Mendes-Victor [a], Amal Sebai [c]

[a] *Centro de Geofísica da Universidade de Lisboa, Edifício C8, Campo Grande, 1749-016 Lisbon, Portugal*
[b] *Instituto Superior de Engenharia de Lisboa, Rua Conselheiro Emídio Navarro, 1950-062 Lisbon, Portugal*
[c] *Institut de Physique du Globe, 4, place Jussieu, 75252 Paris Cedex 05, France*

Received 10 July 2003; accepted 2 March 2006

**Abstract**

The Azores archipelago occupies a lateral branch of the Mid-Atlantic Ridge near the triple junction of three large tectonic plates, the North American, the Eurasian and the African plates. The tectonic setting is even more complex because of the existence of the Azores hotspot and hotspot–ridge interaction. However, the hotspot origin at depth as a plume and its lateral extent are controversial subjects. High-resolution tomographic models, through the mapping of low-velocity and anisotropy anomalies, can provide an important hint to evaluate the depth and lateral extent of plumes when they exist. Therefore, we present a review of the Azores deep seismic structure as inferred from recent global and regional studies. The mapping of S-wave negative velocity anomalies in various models reveals a negative anomaly beneath the Azores confined within the upper 250–300 km. Considering the time evolution of a plume, this low-velocity anomaly might be the signature of a present-day dying plume, which created the Azores plateau 20 Ma ago. However, tomographic investigations have reached the limit of resolution provided by the global and regional seismic coverage available today. Only a long-term deployment (several years) of several broadband seismic stations in the Archipelago and on the surrounding seafloor will provide the increased resolution to better characterize plume geometry.


*Keywords:* Azores; Atlantic Ocean; mantle; hotspot; thermal plume; seismic tomography

## 1. Introduction

The Azores domain comprises a 20-My-old volcanic plateau and an archipelago volcanically active from 7 My to the present. Besides, it is located at the triple junction between the North American, Eurasian, and African plates. In the last, decade a great effort has been made to characterize the geodynamics of the Azores region. However, the source at depth of the long-term volcanism in this area is still debated.

The Azores area is considered by numerous authors to reflect typical ridge–hotspot interaction (e.g., Schilling, 1991), from elevated spreading ridge, basalt geochemistry and gravity anomaly (see Gente et al., 2003, for a recent review). A "hotspot" (Wilson, 1963) is a long-term source of volcanism, which seems relatively fixed compared to the plate overriding it. Its signature on a fast-moving plate is, therefore, a volcanic chain with a well-defined age progression parallel to the plate motion. It is also associated with a bathymetric swell, a gravity

* Corresponding author. Centro de Geofísica da Universidade de Lisboa, Edifício C8, Campo Grande, 1749-016 Lisbon, Portugal.
*E-mail address:* gracams@fc.ul.pt (G. Silveira).

0377-0273/$ - see front matter © 2006 Elsevier B.V. All rights reserved.
doi:10.1016/j.jvolgeores.2006.03.022

anomaly, and basalt geochemistry different from normal mid-ocean ridge basalts. These latter characteristics, as well as an anomalously high volume of volcanism, help define young hotspots, or hotspots on a slow-moving plate, which do not always present a clear age progression. The Azores corresponds to this type, being both young and located on a slow-moving plate.

Since hot thermal plumes are commonly observed in a convecting fluid heated, even partially, from below like the Earth's mantle (e.g., Krishnamurti, 1970; Whitehead and Luther, 1975), it has been proposed that hotspots are the surface signature of thermal plumes originating from a thermal boundary layer located deep in the mantle (Morgan, 1971), either on the core–mantle boundary or in the transition zone. Indeed, the distribution of hotspots compares well with the geoid anomalies and the broad areas of slow seismic velocities (generally interpreted as hot material) seen by tomography in the mantle, with a strong degree 2 distribution in the lower mantle (e.g., Chase, 1979; Anderson, 1982), possibly inducing a degree 6 distribution in the upper mantle (e.g., Cazenave et al., 1989; Cazenave and Thoraval, 1994; Montagner, 1994). Within this framework, volcanism would, therefore, be enhanced at hotspots due to the higher temperature of plumes compared to normal mantle. Higher mantle temperature would produce more partial melting, a thicker crust, and less dense material below the lithosphere. Those two last effects would then explain the topographic swell and gravimetry anomaly observed on hotspots.

Other ways to enhance locally partial melting and, therefore, volcanism could include the presence of a pocket of abnormally hydrated mantle below the lithosphere (e.g., Bonatti, 1990; Asimow and Langmuir, 2003), or by the leakage of an already partially molten mantle through a lithosphere weakened by a complex tectonic setting (Turcotte and Oxburgh, 1973; Anderson, 2000). In those two cases, the bathymetry swell would mainly be produced by the thicker crust, although a higher volatile content might also reduce the mantle density and contribute to the swell.

Since both temperature and volatile-content anomalies, as well as complex tectonics settings are observed on Earth, hotspots of different origins are likely to coexist. Their classification has been attempted in Courtillot et al. (2003). However, to discriminate between the different possible origins of inferred hotspots, seismic tomography is probably one of the most diagnostic tools since it can image the deep structure of the Earth.

Tomographic models enable estimation of physical parameters such as heterogeneities in seismic velocity, anisotropy, attenuation or density at different scales. Such models span the entire depth range of the mantle and can achieve lateral resolutions of 1000 km at a global scale (among others: Grand et al., 1997; Boschi and Dziewonski, 2000; Mégnin and Romanowicz, 2000; Ritsema and van Heijst, 2000). In the upper mantle, regional surface-wave tomography can achieve uniform resolution of about 500–800 km (e.g., Roult and Rouland, 1994; van der Lee and Nolet, 1996; Debayle and Kennett, 2000; Silveira and Stutzmann, 2002). In contrast, body-wave tomography resolution can be locally better (a few hundreds of km), although it is less uniform beneath oceans because it is highly constrained by the uneven station-earthquake distribution (e.g., Bijward and Spakman, 1999; Foulger et al., 2001).

The detection of small-scale geological objects is more problematic. Much progress has been made on the detection of slabs in the mantle (van der Hilst et al., 1997), but the characterization of plumes by seismic tomography is still in its infancy. Although plume conduits may be too narrow to be seen in such models, the expected larger diameter of ponds of plume material beneath the lithosphere should be detectable in high-resolution studies at regional scale as well as at global scale. In the Atlantic Ocean, the global tomographic model of Zhang and Tanimoto (1992, 1993) and the regional tomographic model of Silveira and Stutzmann (2002) display low-velocity anomalies beneath most hotspots of the Atlantic, including the Azores. By using a dedicated seismic network, it was possible to span the entire Iceland area in order to obtain delay-time data that revealed a prominent low-velocity conduit in the upper mantle beneath the island (e.g., Bijward and Spakman, 1999; Foulger et al., 2000, 2001). Along the Mid-Atlantic Ridge, Montagner and Ritsema (2001) recognize two families of hotspots, the first one associated with negative seismic signature no deeper than 300 km and a second one, with Iceland as an example, having seismic signature extending at least down to the transition zone or even deeper. More recently, the model of Montelli et al. (2004) shows a strong slow-velocity anomaly beneath the Azores at 300 km depth that merge with the Canaries anomaly below 1500 km depth. However, their synthetic experiments show that the model lacks resolution in the mid mantle in the Azores area. Hence, the anomaly observed at 300 km depth could be, indeed, located at shallower depth.

As noted by Nataf (2000) in his review paper on seismic imaging of mantle plumes, despite enormous improvements in seismic methods, many questions remain unanswered on the existence of plumes and, if they exist, on their structure, depth origin and

geodynamic role. In this paper, we intend to show how the most recent global and regional tomographic models image the seismic upper mantle structure beneath the Azores and how the role of mantle plumes can be investigated. The Azores pose a very interesting area to understand, since it presents a complex tectonic setting as well as an underlying mantle that has been interpreted as hotter, and more hydrous than normal. After a summary of the surface observations at the Azores (Section 2), we present the upper mantle structure below the Azores, as inferred from recent tomographic studies (Section 3). The results are then interpreted within a fluid mechanics framework (Section 4).

## 2. The Azores region

The Azores plateau lies astride the Mid-Atlantic Ridge (MAR) close to the triple junction where the American, Eurasian and African plates meet (Fig. 1). The MAR separates American plate to the west, and Eurasian and African plates to the east, whereas the boundary between Eurasia and Africa is mainly a transform fault system, i.e., the Azores–Gibraltar Plate boundary zone. The complex morphology of the plateau reflects the interaction of magmatic activity and intense tectonic activity (Ribeiro, 2002). The formation of the plateau began around 20 My and ended around 7 My. The plateau was subsequently rifted from north to south by the Mid-Atlantic Ridge (for a review, see Gente et al., 2003).

The crust beneath the Azores, like the one beneath Iceland and possibly St Paul's Rocks, is thicker than elsewhere along the ridge, reflecting a greater contribution of ultimately mantle-derived liquids (Melson and O'Hearn, 1989). Searle (1976) found a crustal thickness of 8 km from surface-waves dispersion measurements. More recently, the mean crust thickness beneath the Azores was revaluated to be about 9–12 km from elastic plate model estimation (Luis et al., 1998).

The geoid anomaly displays a large asymmetry with a region of high geoid anomaly extending further southwestward along the ridge than it does north of the Azores plateau (e.g., Goslin et al., 1998). The same asymmetry is evident in the geochemical data observed along the ridge (e.g., Dosso et al., 1999). The plateau comprises mainly alkaline basalts. Geochemistry and petrology studies show a source very heterogeneous in isotopic composition, with a high volatile content (Schilling et al., 1980; Bonatti, 1990) and possibly warmer than normal ridge material. Based on uranium-series disequilibrium studies, Bourdon et al. (1996) estimate a 100 °C temperature excess beneath the Azores. Gravimetry data yield an estimate of 75 °C (Cochran and Talwani, 1978) and the elevation of the ridge gives an estimate of 198 °C (Schilling, 1991). Those last two estimates assume that the anomalies

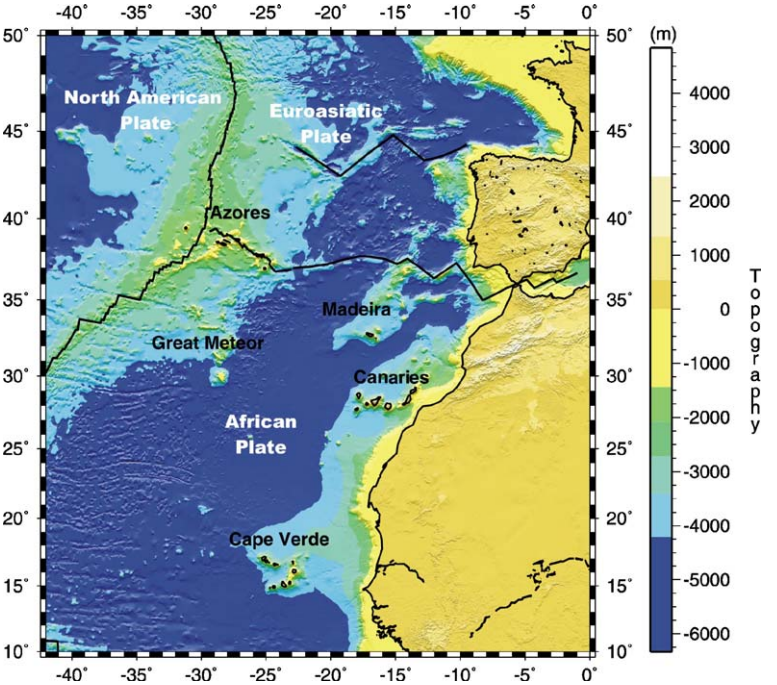


Fig. 1. Bathymetry map of the central east Atlantic Ocean.

are solely due to temperature, and could be reduced if the volatile content is taken into account (e.g., Bonatti, 1990; Asimow and Langmuir, 2003). The relative contributions of excess temperature and volatile content (mostly water) are still heavily debated today. However, if the Azores material is indeed 100–200 °C warmer than normal mantle, then it would be compatible with a plume origin (Schilling, 1975; Schilling et al., 1983).

On top of the plateau has emerged a volcanic archipelago, still active today. Two islands are located west of the ridge axis and seven islands extend up to 550 km east of it. The oldest rocks recovered are 8 My and were found in Santa Maria island. Geochemical data are heterogeneous, but point to the possible coexistence and/or mixing in the source of recycled oceanic crust, Jurassic delamination of continental lithosphere, and undegassed material, high $^3$He, coming from the deep mantle (e.g., Moreira et al., 1999). Based on the rare-gas signature, the Azores hotspot is presently located on the eastern side of the MAR under the central group of islands (see Gente et al., 2003, for a review).

## 3. Tomographic seismic imaging

Tomographic models are derived from different types of measurements involving the recording of an earthquake by seismic stations. Classical tomographic methods use body-wave travel times, surface-wave phase velocities and/or normal-mode frequencies. Body waves are the first phases that are recorded by a station after an earthquake, and they have a dominant period of 1 s for P-waves and 4 s for S-waves. The associated travel times correspond to propagation along rays through the Earth. The seismic signal that arrives after body waves is the most energetic at teleseismic distances and corresponds to the surface-wave train. Surface waves are guided waves that are dispersive and, for studying the mantle, their phase velocities are measured in the period band 40–250 s. Finally, by considering several hour-length seismograms after a strong earthquake, normal modes or eigenfrequencies of the Earth are determined for periods larger than about 150 s. The way of propagation through the Earth and the period domain associated with each type of measurement control the resolution of a tomographic model. Body waves are sensitive to small-scale structures along the rays and the minimum size of a structure that can be recovered is limited by the path coverage, which in turn is controlled by the source and receiver configuration. On the other hand, surface waves sample the mantle along a path epicenter station from the surface down to a depth that depends on the period. The minimum size of the structures that can be recovered using surface waves is about 200 km for a 40-s period measurement and 1000 km for a measurement at 200 s. Therefore, for surface waves the resolution limit is controlled by both the measurement period band and the path coverage.

Body waves, surface waves and normal modes have been extensively used since the mid-1980s for deriving tomographic models. Each measurement is associated with a path through the Earth, and the combination of many crossing paths in a suitable dense source–receiver configuration allows the determination of the shape and amplitude of three-dimensional anomalies with respect to a standard reference model (e.g., PREM model of Dziewonski and Anderson, 1981). This methodology was introduced in the late 1970s (among others: Aki et al., 1977; Dziewonski et al., 1977) and, since then, the number of both global and regional tomographic models using more and more sophisticated methodologies greatly increased (see Romanowicz, 2003, for a recent review on global tomographic models). Nevertheless, depending on the type of data used in the inversion (e.g., body wave versus surface wave), and the model parameterization taking account of anisotropy and anelasticity the resulting tomographic models may provide slightly different images of the Earth.

### 3.1. Global tomographic models

Most recent global tomographic models include both body- and surface-wave data. However, because of the lack of an adequate number of seismic stations and earthquakes, surface waves are the only seismic waves that provide information on the upper mantle structure beneath oceanic areas with uniform resolution. Among the large number of available global models, we have selected three of them for discussion. The first model, SAW24B16 (Mégnin and Romanowicz, 2000), was derived from waveform inversion using an asymptotic theory (Li and Romanowicz, 1996). Waveforms of $S_H$-body waves and fundamental and higher mode Love waves were used to derive an $S_H$-wave velocity model. The second model, S20RTS (Ritsema and van Heijst, 2000) was obtained by inverting body wave travel times ($S_H$, $ScS_H$, SKS, and multiple reflected phases) and Rayleigh surface-wave phase velocities. The authors combined measurements on the transverse and vertical components of the seismogram, but anisotropy was neglected in the inversion for the S-wave velocity model. The third model, SG (Grand et al., 1997), was derived from travel times inversion of $S_H$, $ScS_H$ and multiple reflected phases measured on the transverse

component and the model corresponds to $S_H$-wave velocity perturbations.

In the uppermost 150 km beneath the Atlantic, the three global tomographic models agree that the most prominent feature is the Mid-Atlantic Ridge, associated with a negative velocity anomaly (Fig. 2). Beneath the Azores plateau, we observe, at 100 km depth, an elongated negative anomaly where amplitude is larger than −5% between 35°N and 45°N. This negative anomaly is still visible at 200 km with smaller amplitude but it disappears beneath 300 km depth.

The mapping of seismic velocity anomalies is getting progressively consistent between different global tomographic studies and even with geochemical major elements data (Humler et al., 1993). However, high-resolution global studies have attained the limit in resolution, and the smallest features that can be analysed have diameters on the order of 1000 km. In addition, global models exhibit heterogeneous resolution because of an incomplete data coverage stemming from the uneven source–receiver distribution.

### 3.2. Regional tomographic models

#### 3.2.1. Isotropic S-wave velocity

Whereas global tomographic models mainly discriminate long-wavelength anomalies, small-scale features can only be seen by using regional studies. However, in the Atlantic Ocean, the source–receiver distribution is not well suited for regional tomographic studies.

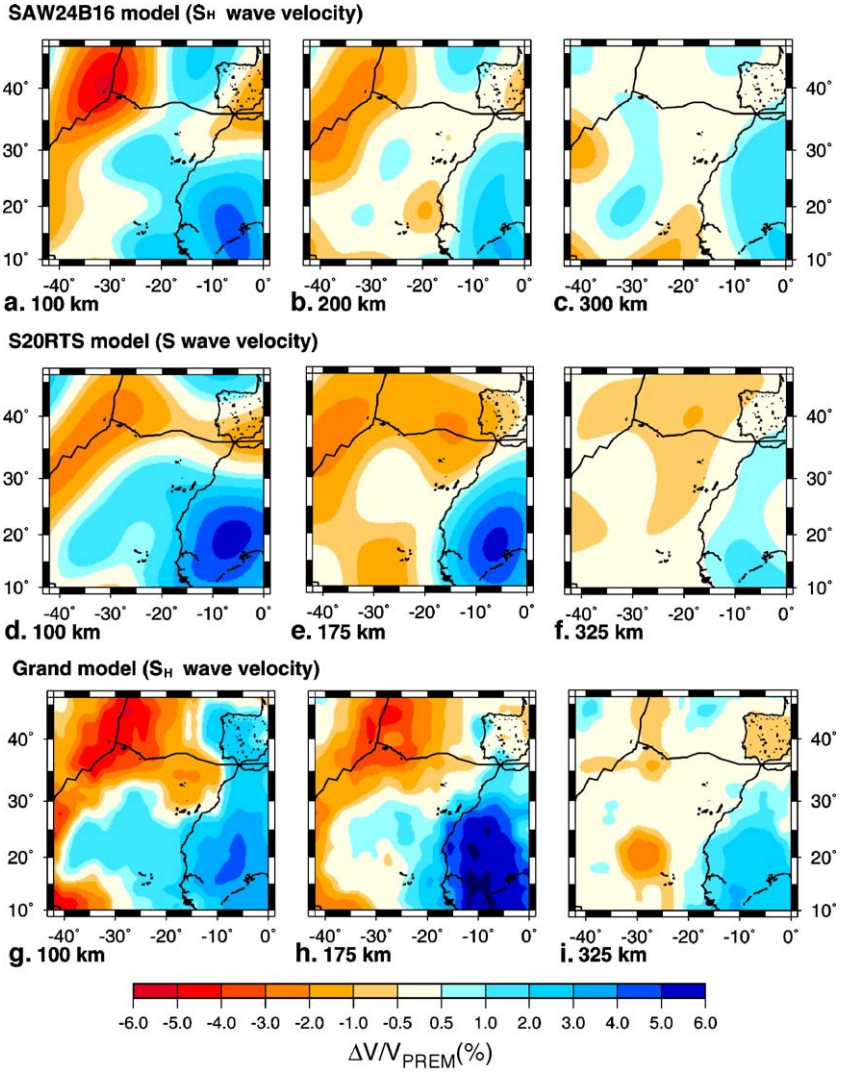


Fig. 2. S-wave velocity perturbations at three depths for three global models. Top row of figures: SAW24B16 model ($S_H$-wave velocity model). Middle row: S20RTS model (S-wave velocity model). Bottom row: Grand's (1994) model ($S_H$-wave velocity model).

Whereas the Pacific Ocean is ringed by seismogenic zones, most of the seismicity around the Atlantic is concentrated in the west American coasts, Mediterranean region and Central Africa. Even the high seismicity of the Mid-Atlantic Ridge is characterized by earthquakes of magnitude smaller than 5.8. So, it is difficult in any tomographic study to isolate the Atlantic Ocean from surrounding continents.

In the mid-1970s and early 1980s, surface-wave dispersion measurements were used to study the average upper mantle structure beneath the entire Atlantic Ocean or parts of it (Weidner, 1974; Canas and Mitchell, 1981; Marillier and Mueller, 1982). Those studies mainly distinguish the Mid-Atlantic Ridge from the ocean basins. Searle (1976) performed local surface-wave dispersion measurements that primarily show that the Azores plateau has a crust with a thickness of about 8 km. The proposed upper mantle structure that fits such observations suggests S-wave velocity not higher than 4.5 km/s.

Honda and Tanimoto (1987) published the first regional tomographic model for the Atlantic Ocean, by surface-wave phase inversion. At shallow depths, they detected the presence of low velocities beneath the Azores triple junction. Mocquet and Romanowicz (1990) inverted Rayleigh wave-phase velocities (Mocquet et al., 1989), to obtain a three-dimensional shear-wave velocity of the upper mantle beneath the Atlantic Ocean. Due to the inhomogeneity of the azimuthal path coverage, the model does not include anisotropy. The lateral resolution of these first regional models is very poor, larger than 2000 km. They found slower velocities beneath the Mid-Atlantic Ridge than beneath ocean basins. Except for the low-velocity anomaly beneath the Azores triple junction (confined to the lithosphere), it is not possible to associate any other negative anomaly with other ridge or near ridge hotspots.

Four years later, Grand (1994), using $S_H$-wave travel times proposed a mantle shear structure beneath the America and surrounding oceans. In the entire upper mantle, it is possible to trace a low-velocity anomaly beneath the Azores, with amplitudes ranging from −4.0%, in the first 100 km, to ∼−1% between 325 and 400 km. However, the vertical extent of the low-velocity anomaly is not well resolved because of the lack of body waves that sample the area.

### 3.2.2. Anisotropic tomographic models

Radial (or polarization) anisotropy and azimuthal anisotropy are two manifestations of the upper mantle anisotropy. Radial anisotropy means that the elastic properties of media differ between horizontal and vertical orientations. This was first inferred from the incompatibility between fundamental mode Love and Rayleigh phase-velocity measurements (Anderson, 1961). Azimuthal anisotropy means that media properties depend on the azimuth, as was first observed by comparing Rayleigh wave-phase velocity measurements along different directions of propagation in the Nazca plate (Forsyth, 1975).

The rapid expansion of broadband seismograph networks during the last two decades of the 20th century have enabled better coverage worldwide, even for poorly sampled regions such as Atlantic. This has made it possible to improve model parameterization by including seismic anisotropy in tomographic methods (Montagner and Nataf, 1986).

Silveira et al. (1998) proposed the first anisotropic Rayleigh wave phase-velocity maps at a regional scale for the Atlantic Ocean. Only the surface-wave fundamental mode was used and, consequently, only the upper 300 km of the mantle could be investigated. The phase velocity maps revealed the presence of a slow-velocity anomaly beneath all the Mid-Atlantic Ridge hotspots up to the largest period inverted (200 , that corresponds roughly to 200–300 km depth) as well as beneath most of Atlantic hotspots. More recently, Silveira and Stutzmann (2002), using Rayleigh and Love wave phase-velocity measurements, derived a model from the Moho down to 300 km depth with a lateral resolution of about 700 km. The tomographic maps display negative S-wave velocity anomalies beneath most of the Atlantic hotspots, from the surface down to 200–300 km depth, confirming the previous interpretation based on phase-velocity maps. All the negative S-wave velocity anomalies associated with the Mid-Atlantic Ridge or near-ridge hotspots are stronger and deeper than the ambient ridge anomalies whose maximum depth is around 150 km. This model was obtained without shallow layer corrections. Crustal layers cannot be recovered using surface waves in the period band 50–250 s but they have an effect on phase velocities even at longer periods (e.g., Stutzmann and Montagner, 1994). Beneath an ocean, a tomographic model without crustal corrections displays higher velocities than after crustal corrections.

The phase-velocity data set used by Silveira and Stutzmann (2002) has been enlarged to about 2500 paths per period to improve the resolution in the Azores area. Crustal corrections have been applied to each path-phase velocity and the inversion procedure is the same as in Silveira and Stutzmann (2002). The new tomographic model is presented in Fig. 3 together with the error maps and a resolution test is presented in the

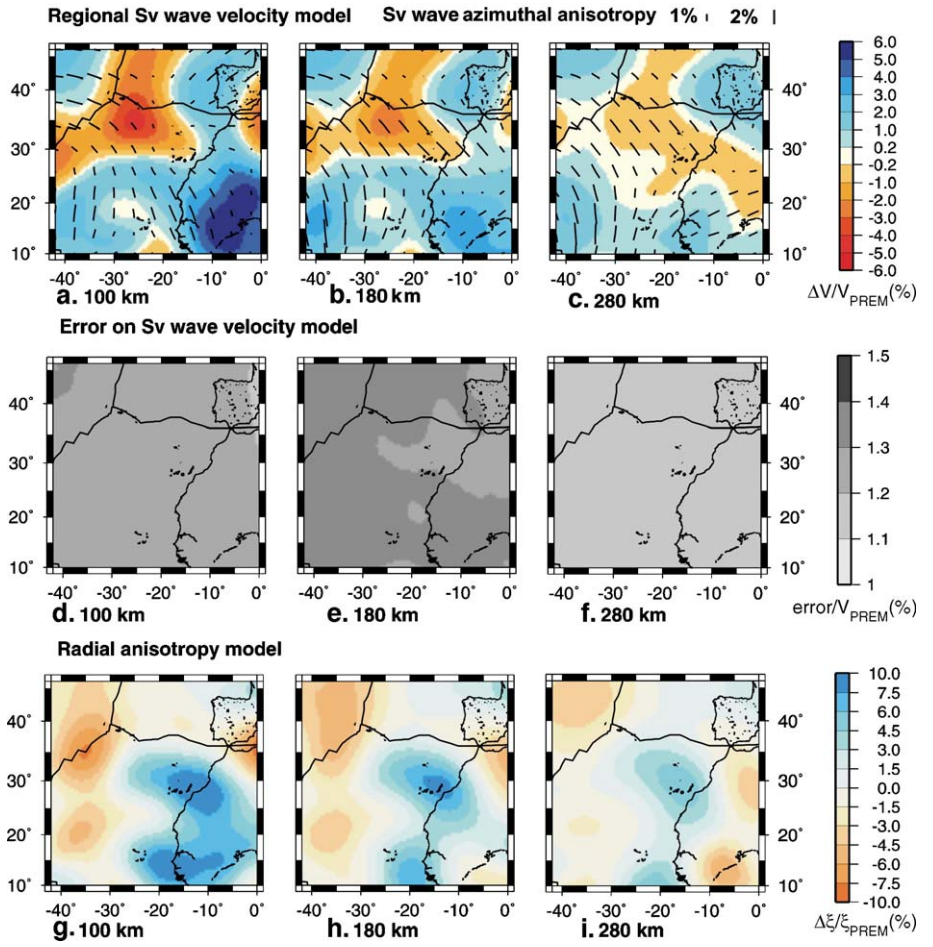


Fig. 3. Regional S-wave velocity model at three depths: 100 km, 180 km and 280 km. Top figures (a–c): $S_V$-wave-velocity model in percent (colour) with respect to the PREM and azimuthal anisotropy fast directions (bars). The bar azimuth gives the S-wave velocity fast direction and its length is proportional to the magnitude. Middle figures (d–f): shows the errors for a–c. Bottom figures (g–i): radial anisotropy lateral variation in percent with respect to PREM.

appendix. As for global models, we retrieve fast velocities beneath the West African craton and slow velocities beneath the Mid-Atlantic Ridge. The path coverage presented in the appendix enables us to sample correctly the area that includes Azores, Great Meteor, Cape Verde and Canaries hotspots and West Africa. Synthetic tests show that if there were three separate anomalies beneath the Azores, Canaries and Cape Verde hotspots having a ray of 200 km and a velocity contrast larger than 3–4% in the upper mantle, they would be seen on the tomographic maps (see the appendix).

The deep structure beneath the Azores is characterized by a broad slow-velocity anomaly clearly visible at 100 km depth. The eastern edges of this low velocity are close to the Great Meteor and Canaries islands. Deeper in the mantle, this slow anomaly remains located beneath the Azores, but its size decreases to disappear around 300 km depth. The anomaly amplitude decreases from −6% at 100 km depth to −3% at 180 km depth and less than −1% at 280 km depth. The associated error maps show that the errors is around 1.1–1.3% in this area at every depth and therefore only anomalies with amplitude larger than ∼±0.5% are significant. Synthetic tests have shown that if there were a plume conduit beneath the Azores deeper than 250–350 km depth with a velocity contrast larger than 3–4% it would be observed on the tomographic map of Fig. 3.

Close to the ridge, the $S_V$-wave azimuthal anisotropy fast directions are perpendicular to the ridge axis (Fig. 3b). Beneath the Azores, the anisotropy fast direction is along a northwest–southeast direction. Radial anisotropy, $\xi$, is plotted as a perturbation with respect to PREM (Fig. 3c).

Radial-anisotropy perturbation is negative beneath the Azores at every depth and its amplitude tends to 0 at 200 km depth. To a first approximation, we have:

$$\xi - 1 \cong 2 \times ((V_{SH} - V_{SV})/V_{SV})$$

The negative radial anisotropy anomaly observed down to 220 km depth means that $S_V$-wave velocity is larger than $S_H$-wave velocity, which can be interpreted as an indication of dominantly vertical flow in this area. Radial anisotropy is derived from the discrepancy between Rayleigh and Love wave-phase velocities. There are less measurements for Love waves than for Rayleigh waves because Love waves are observed on the seismogram horizontal component which is noisier than the vertical component. In this study, we have 3000 paths for Rayleigh waves and 800 for Love waves and, therefore, radial anisotropy cannot be as well resolved as $S_V$-wave velocity and the associate error is around 3–4%.

## 4. Discussion

### *4.1. What is a plume? Cartoons versus fluid-mechanical reality*

Hot thermal plumes are commonly observed in a convecting fluid heated from below (e.g., Krishnamurti, 1970; Whitehead and Luther, 1975). Fig. 4 presents five different stages of such a plume, illustrating its time evolution with a timescale that is normalized to its total lifetime. The plume originates as an instability from the bottom boundary layer with a small head and a small tail (Fig. 4(1)). As it rises, the tail becomes longer and the head grows, being fed by the plume tail (Fig. 4(2)). When the plume reaches the top boundary, it forms a large pond while still remaining connected to the lower boundary by a long conduit (Fig. 4(3)). Then, once the whole contents of the hot thermal boundary layer have been emptied in the instability, the plume tail starts to disappear from the bottom boundary upward and the plume pond reaches its maximum size (Fig. 4(4)). At the end, only the pond below the lithosphere is visible at the top boundary and it is slowly disappearing as the plume cools (Fig. 4(5)). The morphology and the timescales shown here can be altered by rheological and/or compositional effects (e.g., Whitehead and Luther, 1975; Olson and Singer, 1985; Davaille et al., 2003), but a buoyant plume originating from a surface heated from below is a transient phenomena. The first three stages pictured in Fig. 4 have been extensively modelled, using as a proxy a plume produced by a constant ponctual heat source (e.g., Griffiths, 1986). This has given birth to the conventional images of the mantle plume with a broad head and a narrow tail, and/or with a long conduit connecting its source in a bottom thermal boundary layer to the lithosphere. However, as seen in Fig. 5, the latter is valid only during a short time compared with the entire life of the plume. Therefore, because tomographic

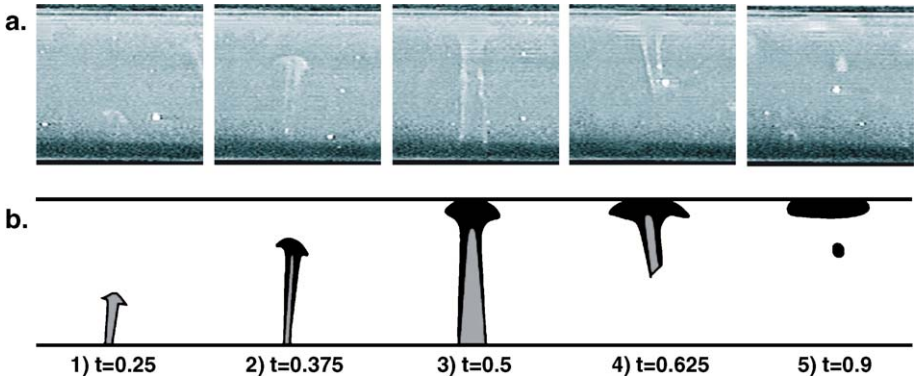


Fig. 4. Temporal evolution of a thermal plume as a function of time (normalized to the total lifetime of the plume). (a) Snapshots from a laboratory experiment in a regime similar to the Earth's mantle (here the Rayleigh number is $2 \times 10^6$): the tank is cooled from above at a temperature $T_0$ and heated from below at temperature $T_0 + \Delta T$. The white line (obtained by illuminating liquid crystals dispersed within the tank) shows the isotherm $0.7 \times \Delta T$; therefore, the white outlines, as an iso-velocity might appear in a tomographic map, reflect the hot plume rising from the hot lower boundary. (b) Sketch outlining the plume seen in the experiment. The black line represents the isotherm while the grey area represents the interior part of the plume with temperature greater than the isotherm. Stages 1 and 2 mark the ascend of the plume through the tank. In stage 3, the plume has impinged the upper boundary and is beginning to spread laterally under it. Stages 4 and 5 illustrate the decline of the plume: stage 4 shows that it has become disconnected from the lower boundary but is continuing to spread under the top boundary. Finally, because at the top boundary the plume is continuously cooling, it loses its once-distinct thermal signature and fades away as shown in stage 5. Note that the full extent of the plume conduit can be seen throughout the whole tank only during a short time (stage 3). With upper mantle properties, the total lifetime of this plume would be 10–40 Ma (Davaille et al., 2002).

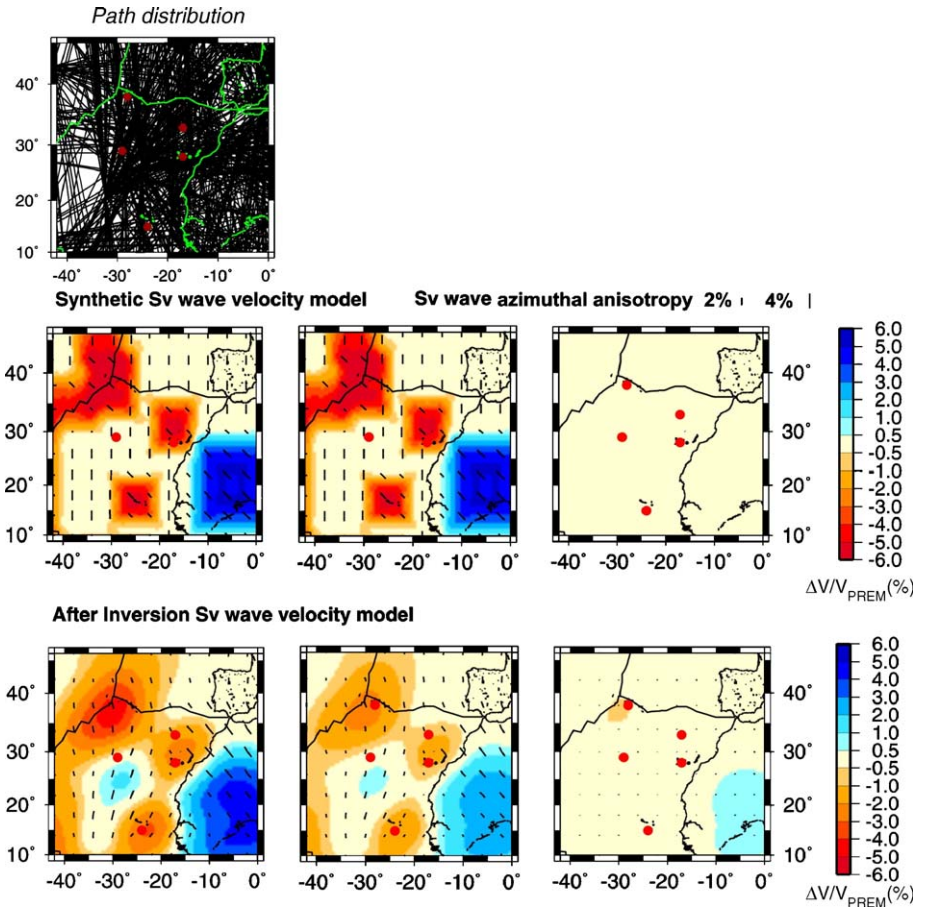


Fig. 5. Test inversion with a synthetic S-wave velocity model at 3 depths: 100 km, 180 km and 280 km. Top figure: geographical path distribution. Middle figures: input $S_V$-wave-velocity model in percent (colour) with respect to the PREM and azimuthal anisotropy fast directions (bars). The bar azimuth shows the S-wave-velocity fast direction and its length is proportional to the magnitude. Bottom figures: after inversion $S_V$-wave velocity model in percent (colour) with respect to the PREM and azimuthal anisotropy fast directions (bars).

images only provide instantaneous present-day images of the mantle, plumes might not be so easy to detect. In particular, it could be erroneous: (1) to link the depth of a present-day slow-seismic anomaly with the depth of its origin, and (2) to interpret the absence of a long tail (Fig. 4(4–5)) as reflecting the absence of a plume.

### 4.2. Dying plume beneath the Azores?

From regional tomographic studies, the deep structure directly beneath the Azores is characterized by a strong broad negative seismic-velocity anomaly clearly visible at 100 km depth but which disappears below 250–300 km depth (Figs. 2 and 3). Collectively, temperature, water content, and partial melting act to decrease seismic wave velocities. The observed negative velocity anomaly above 200 km, therefore, probably corresponds to a combination of the three effects. Since temperature and volatile content also reduce density, the negative seismic anomaly may also indicate more buoyant material that could be produced by a plume. However, the shape of the present-day velocity anomaly beneath the Azores (Figs. 2 and 3) does not correspond to the "cartoon" image of a plume with a broad head followed by a long narrower tail (e.g., Fig. 4(3)), but is more similar to Fig. 4(5), which shows a shallow elongated anomaly. Thus, we could interpret the existence of the anomaly under the Azores, together with the lack of conduit in tomographic models (Figs. 2 and 3), to be a possible signature of the last gasp of a dying plume (i.e., Fig. 4(5)). According to Fig. 4, the Azores basaltic plateau would have been produced when the plume impinged the surface, during stages 3 and 4 of Fig. 4, that is roughly mid-point in the total plume lifetime. As the Azores plateau is 20 My old, we can estimate that the plume lifetime is around 40 My.

## 5. Conclusions

Global and regional tomographic studies show no deep vertical anomaly beneath the Azores, and seem to preclude the present-day existence of a long plume tail there. If it is indeed plume-related, the Azores plateau would, therefore, have been created 20 My ago by a plume which is currently dying. A better understanding of the competing effects of water content, partial melting, and temperature variation on geophysical signals is now required to push the analysis further.

To better characterize the geometry of the low-velocity anomaly, we need a better resolution of tomographic models for the area between the Azores, Great Meteor, Canaries, and Cape Verde, particularly in the 300–1000 km depth zone. This will be achieved only by improving our seismic coverage in the area. The long-term deployment of seafloor broadband seismic stations, combined with permanent land broadband stations on the Azores and Cape Verde islands, seems critical to gain more insight into the mantle dynamics of the Atlantic region.

## Acknowledgments

We thank B. Romanowicz, S. Grand and J. Ritsema for providing their tomographic models. Thanks also to B. Bourdon, M. Cannat, R. Doucelance, M. Maia, M. Moreira, N. Ribe, N. Lourenço and M. A. Moreira for illuminating discussions. Most figures were generated with GMT software. This is an I.P.G.P contribution 2131, UMR CNRS 7580 and 7579. This work was partially sponsored by MASHA (POCTI/CTA/39158/2001), and the CNRS/GRICES cooperation program.

## Appendix A

To assess problems associated with our sampling geometry and to verify the resolution of our model, we carried out a large number of test inversions with synthetic data, using a range of different input models. The path coverage is good in the area that includes the Azores, Great Meteor, Cape Verde, Canaries and East Africa (Fig. 5—top). Fig. 5 also shows one example for a synthetic model with target anomalies located between the surface down to 200 km depth. The slow anomalies are located along the ridge and beneath the hotspots of the Azores, Canaries, and Cape Verde and the fast anomaly is beneath the West African craton. The hotspots maximum negative anomalies have a lateral extent of $2° \times 2°$. After inversion, the location of the target anomalies is recovered well, particularly beneath the Canaries, Cape Verde and West Africa. The anomaly beneath the Azores is also correctly recovered, although it is slightly shifted toward the southeast, which is a consequence of the low number of paths to the east of the Azores due to the weak seismicity in the Atlantic. We observe a smearing of the anomalies and their magnitude is under-estimated in part as a result of the correlation length used in the inversion. The depth extent of the anomalies is correctly retrieved, which means that if there were a plume conduit beneath the Azores having a ray larger than about 150 km and a velocity contrast larger than 3–4%, it would be observed. The synthetic tests also show that if there were three separate anomalies beneath the Azores, Canaries, and Cape Verde hotspots having a ray of about 150–200 km and a velocity contrast larger than 3–4% in the upper mantle, they would be seen on the tomographic map presented in Fig. 3.

## References

Aki, K., Christofferson, A., Huesbye, E.S., 1977. Determination of the three-dimensional structure of the lithosphere. J. Geophys. Res. 82, 277–296.

Anderson, D.L., 1961. Elastic wave propagation in layered anisotropy media. J. Geophys. Res. 66, 2953–2963.

Anderson, D.L., 1982. Hot spots, polar wander, Mesozoic convection and the geoid. Nature 297, 391–393.

Anderson, D.L., 2000. Thermal state of the upper mantle; no role for mantle plumes. Geophys. Res. Lett. 27 (22), 3623–3626.

Asimow, P.D., Langmuir, C.H., 2003. The importance of water to oceanic mantle melting regimes. Nature 421, 815–820.

Bijward, H., Spakman, W., 1999. Tomographic evidence for a narrow whole mantle plume below Iceland. Earth Planet. Sci. Lett. 166, 121–126.

Bonatti, E., 1990. Not so hot "hot spots" in the oceanic mantle. Science 250, 107–111.

Boschi, L., Dziewonski, A.M., 2000. Whole Earth tomography from delay times of P, PcP, PKP phases: lateral heterogeneities in the outer core, or radial anisotropy in the mantle? J. Geophys. Res. 105, 13,675–13,696.

Bourdon, B., Langmuir, C., Zindler, A., 1996. Ridge–hotspot interaction along the Mid-Atlantic ridge between 37°30′ and 40°30′N; the U–Th disequilibrium evidence. Earth Planet. Sci. Lett. 142, 175–189.

Cazenave, A., Thoraval, C., 1994. Mantle dynamics constrained by degree 6 surface topography, seismic tomography and geoid: Inference on the origin of the South Pacific Superswell. Earth Planet. Sci. Lett. 122, 207–219.

Cazenave, A., Souriau, A., Dominh, K., 1989. Global coupling of Earth surface topography with hotspots, geoid and mantle heterogeneities. Nature 340, 54–57.

Canas, J.A., Mitchell, B.J., 1981. Rayleigh wave attenuation and its variation across the Atlantic Ocean. Geophys. J. R. Astron. Soc. 67, 159–176.

Chase, C.G., 1979. Subduction, the geoid, and lower mantle convection. Nature 282, 464–468.

Cochran, J.R., Talwani, M., 1978. Gravity anomalies, regional elevation and the deep structure of the North Atlantic Ocean. J. Geophys. Res. 83, 4907–4924.

Courtillot, V., Davaille, A., Besse, J., Stock, J., 2003. Three distinct types of hotspots in the Earth's mantle. Earth Planet Sci. Lett. 205, 295–308.

Davaille, A., Girard, F., LeBars, M., 2002. How to anchor hot spots in a convecting mantle? Earth Planet. Sci. Lett. 203, 621–634.

Davaille, A., LeBars, M., Carbonne, C., 2003. Thermal convection in a heterogeneous mantle. CRAS Géosciences 335/1, 141–156.

Debayle, E., Kennett, B.L.N., 2000. The Australian continental upper mantle: structure and deformation inferred from surface waves. J. Geophys. Res. 105, 25423–25450.

Dosso, L., Bougault, H., Langmuir, C., Bollinger, C., Bonnier, O., Etoubleau, J., 1999. The age and distribution of mantle heterogeneities along the Mid-Atlantic Ridge (31–41°N). Earth Planet. Sci. Lett. 170, 269–286.

Dziewonski, A.M., Hager, B.H., Oconnell, R.J., 1977. Large-scale heterogeneities in lower mantle. J. Geophys. Res. 82, 239–255.

Dziewonski, A.M., Anderson, D.L., 1981. Preliminary reference Earth model. Phys. Earth Planet. Inter. 25, 297–356.

Forsyth, D.W., 1975. The early structural evolution and anisotropy of the oceanic upper mantle. Geophys. J. R. Astron. Soc. 43, 103–162.

Foulger, G.R., Pritchard, M.J., Julian, B.R., Evans, J.E., Allen, R.M., Nolet, G., Morgan, J.W., Bergsson, B.H., Erlendsson, P., Jakobsdottir, S., Ragnarsson, S., Stefansson, R., Vogfjord, K., 2000. The seismic anomaly beneath Iceland extends down to the mantle transition zone and no deeper. Geophys. J. Int. 142, F1–F5.

Foulger, G.R., Pritchard, M.J., Julian, B.R., Evans, J.E., Allen, R.M., Nolet, G., Morgan, W.J., Bergsson, B., Erlendsson, P., Jakobsdottir, S., Ragnarsson, S., Stefansson, R., Vogfjord, K., 2001. Seismic tomography shows that upwelling beneath Iceland is confined to the upper mantle. Geophys. J. Int. 146, 504–530.

Gente, P., Dyment, J., Maia, M., Goslin, J., 2003. Interaction between the Mid-Atlantic Ridge and the Azores hot spot during the last 85 Myr: emplacement and rifting of the hot spot-derived plateaus. Geochem. Geophys. Geosyst, doi:10.1029/2003GC000527.

Goslin, J., Thirot, J.-L., Noel, O., Francheteau, J., 1998. Slow-ridge/hotspot interactions from global gravity, seismic tomography and Sr-87/Sr-86 isotope data. Geophys. J. Int. 135 (2), 700–710.

Grand, S.P., 1994. Mantle shear structure beneath the Americas and surrounding. J. Geophys. Res. 99, 591–621.

Grand, S.P., van der Hilst, R.D., Widiyantoro, S., 1997. Global seismic tomography; a snapshot of convection in the Earth. GSA Today 7, 1–7.

Griffiths, R.W., 1986. Thermals in extremely viscous fluids, including the effects of temperature-dependent viscosity. J. Fluid Mech. 166, 115–138.

Honda, S., Tanimoto, T., 1987. Regional 3-D heterogeneities by waveform inversion—application to the Atlantic area. Geophys. J. R. Astron. Soc. 94, 737–757.

Humler, E., Thirot, J.-L., Montagner, J.-P., 1993. Global correlations of mid-ocean-ridge basalt chemistry with seismic tomographic images. Nature 364, 225–228.

Krishnamurti, R., 1970. On the transition to turbulent convection. J. Fluid Mech. 42, 295–320.

Li, X.D., Romanowicz, B., 1996. Global shear velocity model developed using non-linear asymptotic coupling theory. J. Geophys. Res. 101, 22245–22272.

Luis, J.F., Miranda, J.M., Galdeano, A., Patriat, P., 1998. Constraints on the structure of the Azores spreading center from gravity data. Mar. Geophys. Res. 20 (3), 157–170.

Marillier, F., Mueller, S., 1982. Structure of the upper mantle in the Northeastern Atlantic close to the Azores–Gibraltar ridge from surface-wave and body-wave observations. Tectonophysics 90, 195–213.

Mégnin, C., Romanowicz, B., 2000. The 3D shear velocity structure of the mantle from the inversion of body, surface and higher mode waveforms. Geophys. J. Int. 143, 709–728.

Melson, W.G., O'Hearn, T., 1989. "Zero-age" variations in the composition of abyssal volcanic rocks. The Geology of North America, Vol. M., The Western North Atlantic Region. The Geological Society of America, pp. 117–136.

Mocquet, A., Romanowicz, B., 1990. Three-dimensional structure of the upper mantle beneath the Atlantic Ocean inferred from long-period Rayleigh waves, II. Inversion. J. Geophys. Res. 95, 6787–6798.

Mocquet, A., Romanowicz, B., Montagner, J.P., 1989. Three-dimensional structure of the upper mantle beneath the Atlantic Ocean inferred from long-period Rayleigh waves, I. Group and phase velocity distributions. J. Geophys. Res. 94, 7449–7468.

Montagner, J-P., 1994. Can seismology tell us anything about convection in the mantle? Rev. Geophys. 32, 115–137.

Montagner, J.-P., Nataf, H.-C., 1986. A simple method for inverting the azimuthal anisotropy of surface waves. J. Geophys. Res. 91, 511–520.

Montagner, J.-P., Ritsema, J., 2001. Interactions between ridges and plumes. Science 294, 1472–1473.

Montelli, R., Nolet, G., Dahlen, F., Masters, G., Hung, S., 2004. Finite frequency tomography reveals a variety of plumes in the mantle. Science 303, 338–343.

Moreira, M., Doucelance, R., Kurz, M.D., Allègre, C.J., 1999. Helium and lead isotope geochemistry of the Azores archipelago. Earth Planet. Sci. Lett. 169, 189–205.

Morgan, W.J., 1971. Convection plumes in the lower mantle. Nature 230, 42–43.

Nataf, H.-C., 2000. Seismic imaging of mantle plumes. Annu. Rev. Earth Planet. Sci. 28, 391–417.

Olson, P., Singer, H., 1985. Creeping plumes. J. Fluid Mech. 158, 511–531.

Ribeiro, A., 2002. Soft Plate and Impact Tectonics. Springer. 324 pp.

Ritsema, J., van Heijst, H.J., 2000. Seismic imaging of structural heterogeneity in Earth's mantle: evidence for large-scale mantle flow. Sci. Progr. 83, 243–259.

Romanowicz, B., 2003. Global mantle tomography: progress status in the last 10 years. Annu. Rev. Geophys. Space Phys. 31 (1), 303.

Roult, G., Rouland, D., 1994. Antarctica I: deep structure investigations inferred from seismology. A review. Phys. Earth Planet. Inter. 84, 15–32.

Schilling, J.G., 1975. Azores mantle blob—rare-earth evidence. Earth Planet. Sci. Lett. 25, 103–115.

Schilling, J.-G., 1991. Fluxes and excess temperatures of mantle plumes inferred from their interaction with migrating mid-ocean ridges. Nature 352, 397–403.

Schilling, J.G., Bergeron, M.B., Evans, R., 1980. Halogens in the mantle beneath the North Atlantic. Philos. Trans. R. Soc. Lond., A 297, 147–178.

Schilling, J.G., Zajac, M., Evans, R., et al., 1983. Petrological and geochemical variations along the Mid-Atlantic Ridge 29-degrees-N to 73-degrees-N. Am. J. Sci. 283 (6), 510–586.

Searle, R.C., 1976. Lithospheric structure of the Azores Plateau from Rayleigh-wave dispersion. Geophys. J. R. Astron. Soc. 44, 537–546.

Silveira, G., Stutzmann, E., 2002. Anisotropic tomography of the Atlantic Ocean. Phys. Earth Planet. Inter. 132, 237–248.

Silveira, G., Stutzmann, E., Griot, D., Montagner, P., Mendes Victor, L., 1998. Anisotropic tomography of the Atlantic Ocean from Rayleigh surface waves. Phys. Earth Planet. Inter. 106, 257–273.

Stutzmann, E., Montagner, J.-P., 1994. Tomography of the transition zone from the inversion of higher mode surface waves. Phys. Earth Planet. Inter. 86 (1–3), 99–115.

Turcotte, D.L., Oxburgh, E.R., 1973. Mid-plate tectonics. Nature 244, 337–339.

van der Hilst, R.D., Widyantoro, S., Engdahl, E.R., 1997. Evidence for deep mantle circulation from global tomography. Nature 386, 578–584.

van der Lee, S., Nolet, G., 1996. Upper mantle *S*-velocity structure of North America. J. Geophys. Res. 102, 22815–22838.

Weidner, D.J., 1974. Rayleigh wave phase velocities in the Atlantic Ocean. Geophys. J. R. Astron. Soc. 36, 105–139.

Whitehead, J.A., Luther, D.S., 1975. Dynamics of laboratory diapir and plume models. J. Geophys. Res. 80, 705–717.

Wilson, J., 1963. A possible origin of the Hawaiian Islands. Can. J. Phys. 41, 863–870.

Zhang, Y.-S., Tanimoto, T., 1992. Ridges, hotspots and their interpretation as observed in seismic velocity maps. Nature 355, 45–49.

Zhang, Y.-S., Tanimoto, T., 1993. High resolution global upper mantle structure and plate tectonics. J. Geophys. Res. 98, 9793–9823.